High-Resolution 2 + 1 REMPI Study of the $a''^1\Sigma_g^+$ State in N_2

E. J. Salumbides, A. Khramov, and W. Ubachs*

Laser Centre, Vrije Universiteit, De Boelelaan 1081, 1081 HV Amsterdam, The Netherlands

Received: October 1, 2008; Revised Manuscript Received: January 9, 2009

We reinvestigated the 2 + 1 REMPI Q-branch spectrum of the $a''^1\Sigma_g^+-X^1\Sigma_g^+$ system of N_2 at around 202 nm in a Doppler-free configuration with counterpropagating laser beams. Highly accurate absolute calibrations were performed using either an I_2 reference standard or a frequency comb reference laser. The observed rotational series shows a clear effect of a perturbation in terms of an anticrossing located at $J = 26$. In addition to the improved set of molecular constants for the $a''^1\Sigma_g^+$ state, we tentatively assign the perturber state to be the $^1\Sigma_g^+$(II) state of N_2.

Introduction

The quantum energy level structure of homonuclear molecules such as N_2 can be subdivided into two noninteracting components, one of gerade and one of ungerade molecular inversion symmetry, defined in the body-fixed frame of the molecule. The connection between the subcompartments is made through electronic dipole-allowed transitions in the spectrum. The level structure of the *u* symmetry excited states has been investigated in detail through classical spectrographic studies, either in absorption[1] or emission,[2] by synchrotron absorption studies,[3] by extreme ultraviolet (XUV) laser studies,[4] and by fragment kinetic energy studies.[5,6] The structure in this *u*-manifold above 100000 cm^{-1} is one of severe complexity. The seemingly erratically ordered singlet states have been unraveled through the semiempirical work of Stahel et al.,[7] who assigned the mutually interacting Rydberg and valence states $^1\Sigma_u^+$ and $^1\Pi_u$ symmetry. Adding to this complex behavior is the coupling of the singlet states to triplet states that causes further perturbations in the level structure as well as predissociation.[8,9]

Prominent quantum states of *g* symmetry, besides the $X^1\Sigma_g^+$ ground state, are the $a^1\Pi_g$ state, observed in the relatively weak Lyman−Birge−Hopfield system[10] and the $a''^1\Sigma_g^+$ state, which is the subject of the present study. The $a''^1\Sigma_g^+$ Rydberg state was first identified via pressure-induced excitation in the dipole-forbidden *g*−*g* transition by Dressler and Lutz.[11] Later Ledbetter identified the $a''^1\Sigma_g^+$ state as the lower level in an infrared emission system, also providing information on the rotational constants.[12] With a combination of pulsed-electron excitation and laser-induced fluorescence, the lifetime of the $a''^1\Sigma_g^+$ state was determined to be 3.49(10) μs;[13] this implies that spectroscopic studies at very high resolution are possible upon excitation of the $a''^1\Sigma_g^+$ state.

2 + 1 resonance enhanced multiphoton ionization (REMPI) on the $a''^1\Sigma_g^+-X^1\Sigma_g^+$ system was performed by a number of groups prior to the present high-resolution study. After an initial study by Lykke and Kay,[14] Hanisco and Kummel[15] improved the resolution and wavelength calibration and also detected the (1,1) and (2,2) bands. Later Rijs et al.[16] performed 2 + 1 REMPI on the $a''^1\Sigma_g^+-X^1\Sigma_g^+$ system, upon photodissociation of N_2O, allowing them to probe the (0, 0) and (1, 1) bands for rotational quantum numbers as high as $J = 94$, albeit at a lower wavelength accuracy.

At higher excitation energies there exist numerous additional states of singlet and gerade symmetry. Kaplan observed the states labeled as $x^1\Sigma_g^-$, $y^1\Pi_g$, and $z^1\Delta_g$, in transitions that are now referred to as the Kaplan systems.[17] More recently de Lange et al.,[18] using a laser-based double-resonance scheme, observed a large number of novel bands and quantum states. Although through the double-resonance scheme the rotational structure could be fully unraveled, the vibronic assignment of the observed structures is still pending.

Ab initio calculations by Ermler et al.[19] predict that there exists a valence state $^1\Sigma_g^+$(II), at much larger internuclear separation than the $a''^1\Sigma_g^+$ state. In the adiabatic potential picture these states of equal symmetry interact and form an $a''^1\Sigma_g^+-{}^1\Sigma_g^+$(II) double-well structure with an outer well minimum at ∼11 eV and an inner well minimum at ∼13 eV. Bominaar et al.[20] recently performed a two-photon excitation study with a powerful tunable excimer-laser system, and they could observe a vibrational level in the outer well, which they tentatively assigned as $v' = 32$. Until now this is the only level observed in the outer well.

In the present study, we reinvestigate the 2 + 1 REMPI spectrum of the $a''^1\Sigma_g^+-X^1\Sigma_g^+(0,0)$ band in N_2 under largely improved resolution and absolute wavelength calibration. The precision obtained allows us to deperturb a local perturbation in the rotational structure of the $a''^1\Sigma_g^+$, $v' = 0$ manifold. However, the information does not allow for an unambiguous identification of the symmetry of the perturber state as either $^1\Sigma_g^+$ or $^1\Pi_g$. We tentatively assign the perturber as a vibrational level in the $^1\Sigma_g^+$(II) outer well state of N_2.

Experimental Methods

The method of 2 + 1 resonance-enhanced multiphoton ionization (REMPI) spectroscopy used in the present experiment is essentially similar to that of previous studies in refs 14−16. However, some features were implemented that allow for higher experimental resolution and accuracy in the experiment. First of all, a laser source was used that delivers laser pulses, tunable near 202 nm, at a much reduced bandwidth of ∼40 MHz. This system, based on an injection-seeded pulsed titanium−sapphire oscillator-amplifier system, and three stages for frequency upconversion, has been documented elsewhere.[21] A crucial improvement is the implementation of 2 + 1 REMPI with counterpropagating laser beams, thus allowing for Doppler-free spectroscopy. The alignment procedure using a Sagnac

* Corresponding author. E-mail: wimu@nat.vu.nl.

10.1021/jp808698u CCC: $40.75
Published on Web 02/18/2009

TABLE 1: Absolute Frequency Positions of $B^3\Pi(0_u^+)-X^1\Sigma_g^+$ Transitions in I_2 Used in the Subsequent N_2 Calibrations[a]

line	position
P125 (0−16) a2	370380996.21 (30)
R134 (0−16) a1	370372289.78 (30)
P135 (0−16) a2	370321305.18 (30)
P127 (0−16) a2	370278962.40 (30)
P128 (0−16) a1	370227354.33 (30)
P211 (0−15) a2	370198437.93 (30)

[a] The positions are listed for the a1 (for even-J) or a2 (for odd-J) hyperfine component, also referred to as the t-component. The values are expressed in megahertz.

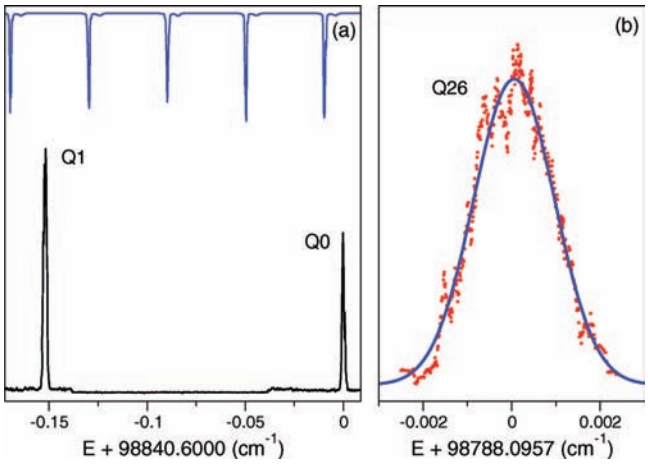

Figure 1. 2 + 1 REMPI spectrum of the $a''^1\Sigma_g^+-X^1\Sigma_g^+(0,0)$ band of N_2. (a) Relative frequency calibrations of the Q(0) and Q(1) transitions using the etalon markers (top trace) with respect to an I_2 resonance (not shown). (b) The absolute frequency calibration of one of the Q(26) transitions, where the maximum perturbative shift occurs, was performed directly against a frequency comb.

interferometer has been applied to produce exactly counter-propagating laser beams.[22] Further methods employed in the present experiment are similar to the ones used in the study of the $EF^1\Sigma_g^+-X^1\Sigma_g^+$ system in H_2 and we refer to that study for all details leading to high resolution and accuracy,[23] in particular including the online frequency-chirp analysis of the pulsed laser.

The absolute calibration was based on a two-step procedure. First, some hyperfine components in the saturated absorption spectrum of the B−X system in I_2, at the fundamental near-infrared wavelength (808 nm), were calibrated at sub-megahertz accuracy against a frequency comb laser that is stabilized against a Rb clock and GPS corrected. Six calibrated I_2 hyperfine resonances, listed in Table 1, were then used as a secondary frequency reference standard during most spectroscopic measurements on N_2. The transmission fringes of an actively stabilized etalon (against a stabilized HeNe laser) provided the relative frequency markers. At the avoided crossing at $J = 26$, absolute frequency calibrations were performed directly using the frequency comb laser, in a similar fashion to previous studies on the calibration of H_2 lines.[23]

Nitrogen molecules were excited downstream in an effusive expansion from a pulsed jet (General Valve). Under normal operation, this yields a low rotational temperature and only the population of the lowest rotational states is found. Varying settings of pulse delays (between nozzle and laser pulses), of nozzle opening times, and of backing pressures made it possible to observe N_2 in rotational quantum states up to $J = 28$.

TABLE 2: Transition Frequencies (in cm^{-1}) As Observed in the $a''^1\Sigma_g^+-X^1\Sigma_g^+(0,0)$ Band of N_2

J	$Q(J)$	J	$Q(J)$
0	98840.6000 (3)	15	98822.3750 (10)
1	98840.4485 (3)	16	98819.9424 (4)
2	98840.1449 (4)	17	98817.3576 (10)
3	98839.6895 (3)	18	98814.6201 (10)
4	98839.0822 (4)	19	98811.7298 (10)
5	98838.3234 (4)	20	98808.6860 (10)
6	98837.4126 (7)	21	98805.4885 (10)
7	98836.3497 (5)	22	98802.1374 (10)
8	98835.1354 (8)	23	98798.6322 (10)
9	98833.7688 (3)	24	98794.9710 (5)
10	98832.2501 (10)	25	98791.1482 (10)
11	98830.5796 (10)	26	98788.09569 (15)[a]
12	98828.7568 (10)	26	98785.74370 (10)[b]
13	98826.7822 (10)	27	98783.1185 (30)
14	98824.6546 (10)	28	98778.8312 (30)

[a] $a''^1\Sigma_g^+$ state: frequency comb calibration. [b] Perturber state: frequency comb calibration.

Results and Discussion

The 2 + 1 REMPI lines of the Q-branch in the $a''^1\Sigma_g^+-X^1\Sigma_g^+$ (0,0) band of N_2 were measured several times and calibrated against the precalibrated hyperfine components in the I_2 reference transitions. Typical spectra of the Q(0) and Q(1) lines are displayed in Figure 1a, demonstrating the improved resolution with respect to previous studies[14,15] in which these Q-branch lines were unresolved. A sample spectrum of the Q(26) transition that was calibrated directly against a frequency comb, is shown in Figure 1b, showing the typical line widths of ∼70 MHz. The result of the calibrated line positions, including the estimated uncertainties, are listed in Table 2. In addition to the Q-branch rotational states from $J = 0$ to 28 of the $a''^1\Sigma_g^+$ state, the $J = 26$ transition belonging to a perturber state was also calibrated; this is the only level associated with the perturber state that is actually observed. The estimated uncertainties for most of the lines were limited by statistics (i.e., the number of measurements). The uncertainties of the two Q(26) lines are significantly smaller than the other transitions on account of the direct calibration.

For the analysis of the spectrum, we adopted a representation for the energy $T_X(J)$ of the rotational levels in the $X^1\Sigma_g^+$, $v'' = 0$ ground state to be

$$T_X(J) = B''[Y] - D''[Y]^2 + H''[Y]^3 \quad (1)$$

with $Y = J(J + 1)$. We used the rotational constants derived by Trickl,[24] from a comprehensive re-evaluation of all available literature on the ground state: $B'' = 1.9895776(10)$ cm^{-1}, $D'' = 5.74137(100) \times 10^{-6}$ cm^{-1}, and $H'' = 4.843(1.000) \times 10^{-12}$ cm^{-1}.

For the $a''^1\Sigma_g^+$, $v' = 0$ excited state we take a similar expression

$$T_{a''}(J) = \nu_{a''(0)} + B'[Y] - D'[Y]^2 \quad (2)$$

with $\nu_{a''(0)}$ representing the band origin.

A perturbation is found to occur in the vicinity of $J = 26$, and we take this perturbation into account in the subsequent analysis. We invoke a perturbing state where its rotational energy levels $T_{pert}(J)$ were calculated using an analogous expression to that of eq 2, following the procedures as described in ref 25, with ν_{pert}, B_{pert}', and D_{pert}'. The effect of the perturbation can be calculated by diagonalizing the matrix for each value of J

$$\begin{pmatrix} T_{a''(0)}(J) & H_{int} \\ H_{int} & T_{pert}(J) \end{pmatrix} \quad (3)$$

A priori, the symmetry of the perturbing state is not known, but in view of the ab initio calculations by Ermler et al.[19] on the $^1\Sigma_g^+$(II) state and the observation of the $v' = 32$ level in this outer well,[20] we assume that the perturbation is due to a lower-lying vibrational level in the outer well. Hence, the perturber is assumed to be of $^1\Sigma_g^+$ symmetry, and in such a case, the interaction is characterized by a homogeneous perturbation where the off-diagonal matrix element H_{int} is independent of rotational quantum number J.[25] We have performed extensive least-squares analyses to extract information on the molecular constants for the a″ state as well as those of the perturber state and the interaction strength parameter H_{int}. For the sake of completeness, we also performed minimization using a heterogeneous perturbation model. This model would represent the perturber state to be of $^1\Pi_g$ symmetry, and the off-diagonal matrix element in this case of a heterogeneous perturbation should be J-dependent: $H_{int} = H'(J(J+1))^{1/2}$.

In the fitting procedures, we chose to fix the ground-state molecular constants to the accurately known values of ref 24, since each ground rotational state is accessed once (except for $J = 26$) for the Q-branch series; thus in reality, we can only access the difference of the upper and lower state constants. In addition, the small size of the data set limits the number of variable parameters that can be used. Nevertheless, after the optimum parameter set for the upper states was obtained, we tried to vary the ground-state parameters (keeping the other parameters fixed) but this did not yield any improvements in the goodness of fit.

The perturbative shifts ΔE are calculated by subtracting the perturbed level energies from the unperturbed $a''^1\Sigma_g^+$ series using the constants of Table 3 and setting $H_{int} = 0$. The resulting perturbative shifts are displayed in Figure 2, yielding a clear graphical representation of the avoided crossing. The relatively weak interaction causes shifts of <0.03 cm^{-1} except at $J = 26$, where the shift amounts to 0.8 cm^{-1}. This marked offset at $J = 26$ had already been observed by Hanisco and Kummel.[15] The quality of the present experimental results makes it possible to see the subtle progression of the shifts starting already at $J = 15$.

The results from the least-squares fit are collected in Table 3 for both cases of a homogeneous and a heterogeneous perturbation. Despite the high accuracy of the data, it was not possible to determine which of the two models is best suited to describe the perturber state. In both models convergence to $\chi^2 \approx 8$ was achieved, which is very satisfactory for a fit with over 20 degrees of freedom. Highly accurate molecular parameters for the $a''^1\Sigma_g^+$ state are obtained, as well as a highly accurate value for the interaction parameter H_{int}. However, the parameters for the perturber state (ν_{pert}, B_{pert}', and D_{pert}') exhibit extremely strong

TABLE 3: Obtained Molecular Parameters for the $a''^1\Sigma_g^+$ State of N_2 (in cm^{-1}), and the Value for the Interaction Parameter with a Perturber State[a]

	homogeneous	heterogeneous	ref 15
$\nu_{a''(0)}$	98840.60189 (15)	98840.59993 (15)	98840.59 (12)
B'	1.9137062 (15)	1.9137062 (15)	1.9143 (2)
D'	6.0000 (25) × 10^{-6}	6.0000 (25) × 10^{-6}	6.6 (2) × 10^{-6}
H_{int}	1.13933 (17)	0.043020 (6)	

[a] Calculations are performed with the assumption of perturber state of $^1\Sigma_g^+$ (homogeneous interaction) or of $^1\Pi_g$ (heterogeneous interaction) symmetry. We also include the values obtained by Hanisco and Kummel[15] for comparison.

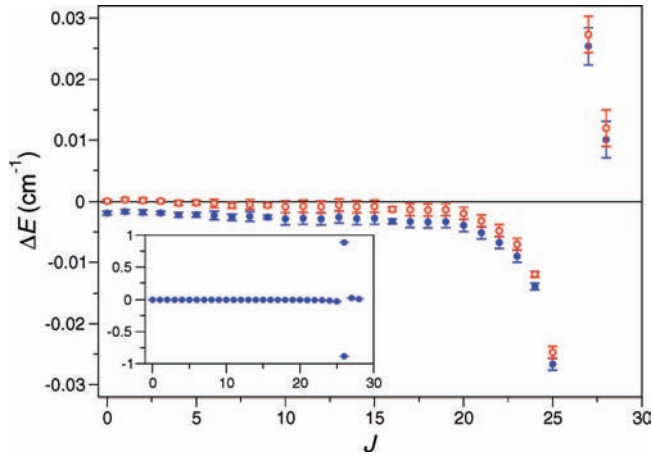

Figure 2. The perturbative shifts on the Q-branch transitions of $a''^1\Sigma_g^+ - X^1\Sigma_g^+(0,0)$ system. The filled circles (blue) represent the shifts in the case of a homogeneous perturbation while the unfilled circles (red) represent those in the case of heterogeneous perturbation. The inset shows an overview to include the $J = 26$ transitions, with the upper point representing the transition belonging to the perturber state.

correlations, while the error landscape is riddled with a great number of local minima close to $\chi^2 \approx 8.3$. This gives rise to a dependence of the least-squares fit on the starting values, in particular for the band origin ν_{pert}. For starting values of ν_{pert} in the wide range of 99100−99900 cm^{-1} the lowest local minimum was found near $\nu_{pert} = 99502$ cm^{-1}. However, the neighboring local minima ($\nu_{pert} = 99495-99505$ cm^{-1}) in the error landscape do not differ at a statistically significant level ($\Delta\chi^2 < 0.01$). Hence, we conclude that we cannot unambiguously determine the symmetry of the perturber nor a reliable value for the band origin. At the lowest minimum with $\chi^2 = 8.3$, we obtain $\nu_{pert} = 99502.31(1)$ and $B_{pert}' = 0.96606(2)$, where we have fixed D_{pert}' to zero since the inclusion of this parameter does not significantly lower the χ^2 value.

This result is somewhat surprising, when comparing with the analysis of a perturbation in the $K^1\Sigma^+$, $v = 0$ state of $^{13}C^{18}O$, in which 28 quantum levels were detected at an accuracy of only 0.05 cm^{-1}.[25] That analysis resulted in an unambiguous identification of the symmetry of the perturber and an accurate determination of molecular constants of the perturber state, even without having observed a single level of that perturber. In the present example, level energies are determined at almost 2 orders of magnitude higher accuracy, and in addition, one perturber level has been detected (at $J = 26$). The strength of the interaction for the example of ref 25 is much larger ($H_{int} = 1.018$ cm^{-1} for a heterogeneous perturbative interaction) and the band origins are closer, resulting in 27 levels with shifts much greater than the experimental uncertainty. We conclude that this strong interaction imparts more information about the perturber state and thus convergence toward a global minimum is possible in the case of ref 25, whereas it is not possible in the present example.

Bominaar et al.[20] have calculated level energies for a sequence of vibrational levels in the $a''^1\Sigma_g^+ - {}^1\Sigma_g^+$(II) double-well potential obtained from ab initio calculations by Ermler et al.[19] They have tentatively assigned the $v' = 32$ level to the band origin found at 103621 cm^{-1}, while the calculations yield $\nu_{32} = 103497$ and $\nu_{33} = 103876$ cm^{-1}. In the calculations of ref 20, a prediction is made for vibrational level energies of $\nu_{22} = 99239$ cm^{-1} and $\nu_{23} = 99839$ cm^{-1}. In the present analysis we cannot determine unambiguously the symmetry of the perturber state, but in view of the fact that vibrational levels pertaining to $^1\Sigma_g^+$(II) must

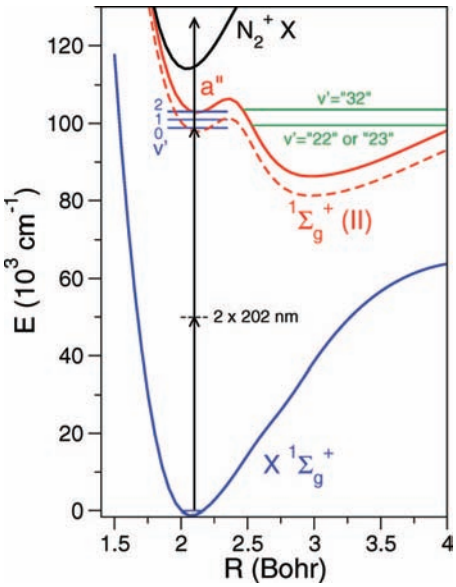

Figure 3. Potential energy curves for N_2. In the adiabatic picture, a double-well potential is formed from the interaction of the $a''^1\Sigma_g^+$ and $^1\Sigma_g^+$(II) states. While the solid curve for the $a''^1\Sigma_g^+$(II) represents the data from Ermler et al.,[19] the dashed curve is the potential that was shifted down by Bominaar et al.,[20,26] to match the a″(0) level with observations. The horizontal lines indicate the experimentally observed energy levels.

exist in this energy range, we tentatively assign the observed perturber state to either $v' = 22$ or $v' = 23$.

The comparison of the experimental results and the calculated band origins in ref 20, based on the ab initio potential of Ermler et al.,[19] strongly suggests that the potential is far from spectroscopic accuracy. For clarity, we have reproduced the ab initio potential,[19] including the experimentally determined[15,20] levels in Figure 3. The $a''^1\Sigma_g^+$ $v' = 1$ level is predicted at 100827 cm^{-1} (with $B' = 1.442$ cm^{-1}), while the experimentally determined value of the $a''^1\Sigma_g^+$ $v' = 1$ level energy[15,24] is 100985.2(2) cm^{-1} (with $B' = 1.882(1)$ cm^{-1}). In fact, both the observed $a''^1\Sigma_g^+$ $v' = 0$, 1 levels are below the minimum of the inner part of the calculated potential energy curve. Indeed, this discrepancy has been noted Bominaar et al.,[20] where they have set the $a''^1\Sigma_g^+$(II) $v' = 21$ level to be identical to $a''^1\Sigma_g^+$ $v' = 0$, to arrive at the values indicated in Table 2 of ref 20. This global offset effectively shifts the $a''^1\Sigma_g^+$(II) potential down[26] by 5012 cm^{-1} as indicated by the dashed curve in Figure 3. However, this correction is not entirely satisfactory, since the $a''^1\Sigma_g^+$ $v' = 2$ level (experimental level energy[15,24] at 103090.0(2) cm^{-1}) is then above the potential barrier. This contradicts the experimental results for the rotational constant $B' = 1.820(1)$ cm^{-1} from ref 15, which clearly indicate that the $v' = 2$ level should be confined inside the inner well. It is then not surprising that the band origins of the outer well, for example in Bominaar et al.[20] as well as the perturber state in the present experiment, do not coincide with the predicted values. Improved ab initio calculations of the $^1\Sigma_g^+$ potentials should help in clarifying these issues.

Summary and Conclusions

We have performed a high-resolution reinvestigation of the $a''^1\Sigma_g^+ - X^1\Sigma_g^+$ system of N_2. The accuracy of most two-photon Q-branch lines at ≤ 0.001 cm^{-1} shows a clear effect of a perturbation with a maximum shift at $J = 26$. However, the interaction is relatively weak, such that even with the present accuracy we cannot satisfactorily resolve the issue of whether the perturber state is of $^1\Sigma_g^+$ or of $^1\Pi_g$ symmetry. On the basis of the fact that the $^1\Sigma_g^+$(II) state is known to exist in this energy range, we tentatively assign the perturber as either $v' = 22$ or $v' = 23$ of this outer well state of N_2.

Acknowledgment. We thank Dr. G. C. Groenenboom for clarifications on the ab initio calculations of the band origins and the referees for their helpful remarks. This research was supported by The Netherlands Foundation for Fundamental Research of Matter (FOM).

References and Notes

(1) Carroll, P. K.; Collins, C. P. *Can. J. Phys.* **1969**, *47*, 563.
(2) Ajello, J. M.; James, G. K.; Franklin, B. O.; Shemansky, D. E. *Phys. Rev. A* **1989**, *40*, 3524.
(3) Stark, G.; Huber, K. P.; Yoshino, K.; Smith, P. L.; Ito, K. *J. Chem. Phys.* **2005**, *123*, 214303.
(4) Ubachs, W.; Tashiro, L.; Zare, R. N. *Chem. Phys.* **1989**, *130*, 1.
(5) Walter, C. W.; Cosby, P. C.; Helm, H. *J. Chem. Phys.* **1993**, *99*, 3553.
(6) van der Kamp, A. B.; Cosby, P. C.; van der Zande, W. J. *Chem. Phys.* **1994**, *184*, 319.
(7) Stahel, D.; Leoni, M.; Dressler, K. *J. Chem. Phys.* **1983**, *79*, 2541.
(8) Lewis, B. R.; Gibson, S. T.; Zhang, W.; Lefebvre-Brion, H.; Robbe, J.-M. *J. Chem. Phys.* **2005**, *122*, 144302.
(9) Vieitez, M. O.; Ivanov, T. I.; Ubachs, W.; Lewis, B. R.; de Lange, C. A. *J. Mol. Liq.* **2008**, *141*, 110.
(10) Vanderslice, J. T.; Tilford, S. G.; Wilkinson, P. G. *Astrophys. J.* **1965**, *141*, 395.
(11) Dressler, K.; Lutz, B. L. *Phys. Rev. Lett.* **1967**, *19*, 1219.
(12) Ledbetter, J. W. *J. Mol. Spectrosc.* **1972**, *42*, 100.
(13) Kam, A. W.; Pipkin, F. M. *Phys. Rev. A* **1991**, *43*, 3279.
(14) Lykke, K. R.; Kay, B. D. *J. Chem. Phys.* **1989**, *90*, 7602.
(15) Hanisco, Th. F.; Kummel, A. C. *J. Phys. Chem.* **1991**, *95*, 8565.
(16) Rijs, A. M.; Backus, E. H. G.; de Lange, C. A.; Janssen, M. H. M.; Wang, K.; McKoy, V. *J. Chem. Phys.* **2001**, *114*, 9413.
(17) Kaplan, J. *Phys. Rev.* **1935**, *47*, 259.
(18) de Lange, A.; Lang, R.; van der Zande, W.; Ubachs, W. *J. Chem. Phys.* **2002**, *116*, 7893.
(19) Ermler, W. C.; Clarck, J. P.; Mulliken, R. S. *J. Chem. Phys.* **1986**, *86*, 370.
(20) Bominaar, J.; Schoemaecker, C.; Dam, N.; ter Meulen, J. J.; Groenenboom, G. C. *Chem. Phys. Lett.* **2007**, *435*, 242.
(21) Hannemann, S.; van Duijn, E.-J.; Ubachs, W. *Rev. Sci. Instrum.* **2007**, *78*, 103102.
(22) Hannemann, S.; Salumbides, E. J.; Ubachs, W. *Opt. Lett.* **2007**, *32*, 1381.
(23) Hannemann, S.; Salumbides, E. J.; Witte, S.; Zinkstok, R.; van Duijn, E.-J.; Eikema, K. S. E.; Ubachs, W. *Phys. Rev. A* **2006**, *74*, 062514.
(24) Trickl, T.; Proch, D.; Kompa, K. L. *J. Mol. Spectrosc.* **1995**, *171*, 374.
(25) Eikema, K. S. E.; Hogervorst, W.; Ubachs, W. *J. Mol. Spectrosc.* **1994**, *163*, 19.
(26) Groenenboom, G. C. Private communication, 2008.

JP808698U